

## Design rules to achieve high- $T_C$ ferromagnetism in (Ga, Mn)As alloys

This article has been downloaded from IOPscience. Please scroll down to see the full text article.

2007 J. Phys.: Condens. Matter 19 242203

(<http://iopscience.iop.org/0953-8984/19/24/242203>)

View [the table of contents for this issue](#), or go to the [journal homepage](#) for more

Download details:

IP Address: 129.252.86.83

The article was downloaded on 28/05/2010 at 19:13

Please note that [terms and conditions apply](#).

## FAST TRACK COMMUNICATION

## Design rules to achieve high- $T_C$ ferromagnetism in (Ga, Mn)As alloys

A Franceschetti<sup>1</sup>, A Zunger<sup>1</sup> and M van Schilfgaarde<sup>2</sup><sup>1</sup> National Renewable Energy Laboratory, Golden, CO 80401, USA<sup>2</sup> University of Arizona, Tempe, AZ 85287, USA

Received 5 April 2007

Published 24 May 2007

Online at [stacks.iop.org/JPhysCM/19/242203](http://stacks.iop.org/JPhysCM/19/242203)

### Abstract

The Curie temperature  $T_C$  of ferromagnetic semiconductor alloys depends not only on the alloy composition, but also on the spatial configuration of the magnetic impurities. Here we use a set of first-principle-calculated Curie temperatures to uncover—via a statistical, ‘data mining’ approach—the rules that govern the dependence of  $T_C$  on the configuration of Mn substitutional impurities in GaAs. We find that  $T_C$  is lowered (raised) when the average number of first (third and fourth) nearest-neighbour Mn pairs increases, suggesting simple atom-by-atom strategies to achieve high  $T_C$  in (Ga, Mn)As alloys.

(Some figures in this article are in colour only in the electronic version)

The physical properties of compounds and alloys often depend not only on their chemical composition, but also, for a given composition, on the fashion in which lattice sites are ‘decorated’ by various atom types. This structural dependence is exemplified by the different properties of various ‘polytypes’ of semiconductor compounds, such as SiC [1], and by the notable changes in the properties of semiconductor alloys upon ordering or superlattice formation [2]. Another example is the ferromagnetic Curie temperature  $T_C$  of (Ga, Mn)As alloys, where Mn impurities substitute for Ga atoms. Depending on the spatial configuration of the Mn impurities,  $T_C$  can range from 0 to over 300 K [3, 4]. The wide range of Curie temperatures attainable at fixed Mn concentration offers the possibility of tuning  $T_C$  by artificially manipulating the configuration of the magnetic impurities. Indeed, atom-by-atom substitution of individual Ga atoms by Mn atoms in GaAs has been demonstrated recently by Kitchen *et al* [5] using a scanning tunnelling microscope. Following the predictions of Mahadevan *et al* [6, 7], the authors found a strong dependence of Mn–Mn ferromagnetic interactions on the crystallographic orientation of the Mn–Mn pairs, and proposed that the Curie temperature of the random alloy can be exceeded by growing ordered (Ga, Mn)As structures [5].

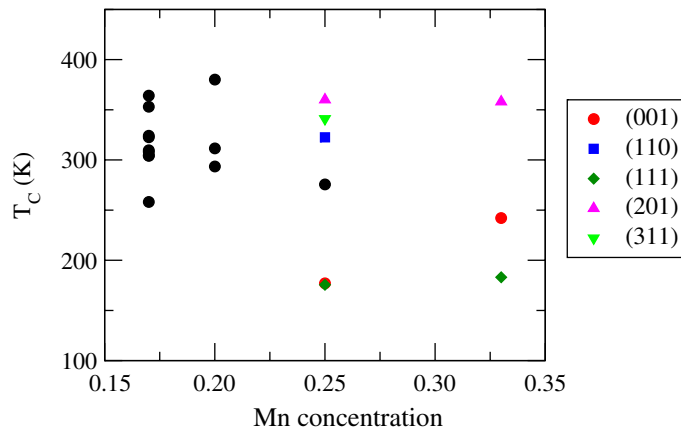


**Figure 1.** Curie temperature of the 21 (Ga, Mn)As ordered structures included in the input set  $\{\sigma_{\text{input}}\}$ , calculated from Monte Carlo simulations of the Heisenberg Hamiltonian. Different symbols denote different orientations of short-period (Ga, Mn)As superlattices.

Exploring the space of possible configurations of the magnetic impurities in search of those that maximize  $T_C$ , however, would be extremely time-consuming, because of the astronomical number of possibilities. In a previous work [3], we used the cluster expansion method [8] to explore a large number of spatial configurations of Mn impurities in GaAs. We found that the highest- $T_C$  structures are ordered GaAs/MnAs superlattices in the (201) crystallographic orientation. In the present work we use a set of first-principle-calculated Curie temperatures to uncover—via a statistical, ‘data mining’ approach—the rules that govern the dependence of  $T_C$  on the configuration of Mn substitutional impurities in GaAs. We find that  $T_C$  is lowered (raised) when the average number of first (third and fourth) nearest-neighbour Mn pairs increases. Our approach offers simple atom-by-atom strategies to achieve high  $T_C$  in (Ga, Mn)As alloys.

The Curie temperature  $T_C(\sigma)$  of an arbitrary configuration  $\sigma$  of Mn substitutional impurities in GaAs is calculated using the best strategies available. (i) The electronic structure of the configuration  $\sigma$  is obtained from density-functional theory in the local-density approximation. (ii) For each configuration  $\sigma$ , the exchange interactions  $\{J_{ij}(\sigma)\}$ —which enter the Heisenberg Hamiltonian  $H = -\sum_{i,j} J_{i,j}(\sigma) s_i \cdot s_j$ —are calculated directly from linear response theory (LRT) [9]. In general, we find that the  $J_{i,j}(\sigma)$  are non-monotonic as a function of the  $i-j$  distance, depend on the crystallographic orientation of the  $i-j$  Mn pair, and extend up to  $\sim 15$  nearest-neighbour shells. (iii) For each configuration  $\sigma$ , we calculate  $T_C(\sigma)$  using a Monte Carlo (MC) simulation of the Heisenberg Hamiltonian<sup>3</sup>. For a random substitutional alloy ( $x_{\text{Mn}} = 8\%$ ) our procedure yields  $T_C = 230$  K, this being an upper bound to the currently measured value  $T_C \approx 160$  K [10] for a nearly uncompensated (Ga, Mn)As alloy. Clustering effects present in currently grown samples can be responsible for the lower-than-ideal  $T_C$  [11].

Using the method described above, we calculated  $T_C$  for an input set of 21 ordered structures  $\{\sigma_{\text{input}}\}$  (see figure 1 and table 1) that includes all  $\text{Ga}_n\text{Mn}_m\text{As}_{n+m}$  supercells with  $n + m \leq 6$  and Mn composition  $1/6 \leq x_{\text{Mn}} \leq 1/3$ . We see from figure 1 and table 1 that  $T_C$  depends not only on the Mn composition but also, at each composition, on the configuration

<sup>3</sup> We use a simulation cell of up to  $8 \times 8 \times 8$  or  $10 \times 10 \times 10$  times the unit cell used to calculate  $\{J_{ij}(\sigma)\}$ . The number of MC steps ( $\sim 10^4$ – $10^5$ ) and the number of independent MC runs are systematically increased until the statistical error bars of the cumulants allow us to determine  $T_C$  to within  $\sim 3$  K.

**Table 1.** Calculated Curie temperature  $T_C$ , Mn concentration  $x_{\text{Mn}}$ , and parameters  $N_R$  (for  $R = \text{NN}_1 \dots \text{NN}_4$ ) of the (Ga, Mn)As structures included in the input set  $\{\sigma_{\text{input}}\}$ .

Structure	$T_C$ (K)	$x_{\text{Mn}}$	$\text{NN}_1$	$\text{NN}_2$	$\text{NN}_3$	$\text{NN}_4$
1	304	0.17	2	0	2	6
2	258	0.17	2	2	4	2
3	304	0.17	2	0	2	6
4	309	0.17	2	0	0	4
5	322	0.17	0	4	0	4
6	353	0.17	0	2	4	2
7	364	0.17	0	0	8	2
8	324	0.17	2	0	2	6
9	308	0.17	2	0	4	2
10	293	0.20	2	2	4	2
11	311	0.20	2	0	4	2
12	380	0.20	0	2	8	0
13	175	0.25	6	0	6	6
14	341	0.25	2	0	6	6
15	177	0.25	4	4	0	4
16	360	0.25	0	4	8	4
17	275	0.25	0	6	0	12
18	322	0.25	2	2	4	4
19	242	0.33	4	4	0	4
20	358	0.33	2	2	12	2
21	183	0.33	6	0	6	6

of the Mn impurities. For example, figure 1 shows that  $T_C$  is larger for GaAs/MnAs (201) superlattices than for (001) or (111) superlattices with the same Mn composition.

In the next step, we randomly select a subset of the input set,  $\{\sigma_{\text{fit}}\} \subset \{\sigma_{\text{input}}\}$ , which includes 15 of the 21 structures in  $\{\sigma_{\text{input}}\}$ . We then fit the  $T_C(\sigma)$  of the structures in  $\{\sigma_{\text{fit}}\}$  using the expansion

$$T_C(\sigma) = t_0 + \sum_R t_R N_R(\sigma), \quad (1)$$

where  $t_0$  and  $\{t_R\}$  are fitting parameters<sup>4</sup>, and  $N_R(\sigma)$  is the number of Mn–Mn pairs separated by the face-centred cubic (fcc) lattice vector  $\mathbf{R}$ , divided by the number of Mn atoms, in the configuration  $\sigma$ . The remaining six structures in  $\{\sigma_{\text{input}}\}$  are used as a benchmark to test the predictive capability of equation (1). We include in the expansion of equation (1) the set of lattice vectors  $\{\mathbf{R}\}$  corresponding to the first four fcc nearest-neighbour pairs ( $\text{NN}_1 \dots \text{NN}_4$ ) on the cation sublattice, as shown in figure 2. Note that the  $\text{NN}_1$  and  $\text{NN}_4$  pairs are oriented in the (1, 1, 0) crystallographic direction, which is characterized by chains of alternating cations and anions (see figure 2), while the  $\text{NN}_2$  pair is oriented along the (0, 0, 1) direction and  $\text{NN}_3$  is along the (2, 1, 1) direction.

The expansion coefficients of equation (1) are fitted to the calculated  $T_C$ s of the structures in the set  $\{\sigma_{\text{fit}}\}$  using a least-squares fitting algorithm. The results are summarized in table 2. Considering the large range of  $T_C$  of the structures in the input set (see figure 1), and the small number of fitting parameters, the quality of the fit (error = 24 K) is rather good. We find that the quality of the fit improves only marginally if more fcc pairs are included in the

<sup>4</sup> The fitting parameter  $t_0$  should not be construed as the value of  $T_C$  in the limit  $x_{\text{Mn}} \rightarrow 0$ , because all the structures considered here are in the composition range  $16\% < x_{\text{Mn}} < 34\%$ .

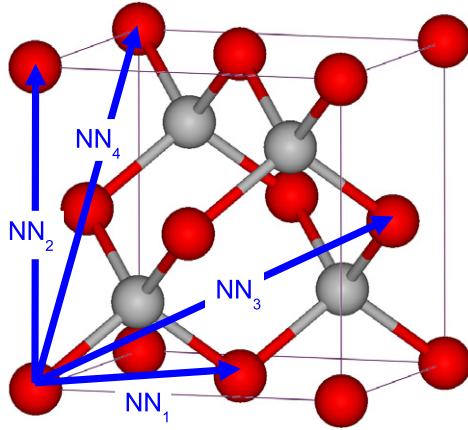


**Figure 2.** First four nearest-neighbour vectors on the cation fcc sub-lattice (arrows). Ga/Mn atoms are denoted by red (dark grey) circles, while As atoms are denoted by light grey circles.

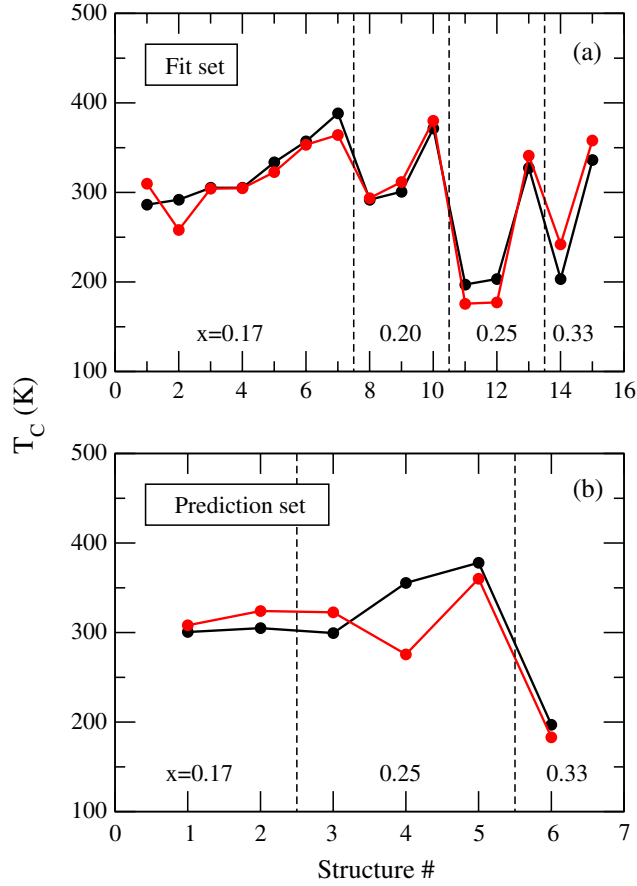
expansion of equation (1). Figure 3(a) compares the directly calculated (by LRT + MC)  $T_C$  of the structures in  $\{\sigma_{\text{fit}}\}$  with the values obtained from equation (1). Figure 3(b) compares the directly calculated  $T_C$  of the structures *not* included in  $\{\sigma_{\text{fit}}\}$  with the value predicted from equation (1). The standard deviation is  $\sim 38$  K.

The main conclusions that are apparent from the results of the fit (see table 2) are that the coefficient  $t_{(1/2,1/2,0)}$  (corresponding to  $\text{NN}_1$ ) is negative and large and the coefficient  $t_{(0,0,1)}$  ( $\text{NN}_2$ ) is small and negative, whereas the coefficients  $t_{(1,1/2,1/2)}$  and  $t_{(1,0,1)}$  ( $\text{NN}_3$  and  $\text{NN}_4$ ) are relatively small and positive. This means that structures with no first-nearest-neighbour Mn–Mn pair ( $t_{(1/2,1/2,0)} = 0$ ) tend to have the highest  $T_C$ , whereas structures with  $t_{(1/2,1/2,0)} = 4$  or 6 have the lowest  $T_C$ . *This result suggests that the main route to achieving high- $T_C$  ferromagnetism in uncompensated, Mn-doped GaAs is to prevent the formation of Mn–Mn first-nearest-neighbour pairs, while at the same time maintaining a sufficiently large Mn concentration by allowing for third and fourth Mn pairs.*

**Table 2.** Coefficients of the expansion of equation (1), obtained from a least-squares fit of the structures included in  $\{\sigma_{\text{fit}}\}$ .

Parameter (equation (1))	$T$ (K)
$t_0$	335.6
$t_{(1/2,1/2,0)}$ ( $\text{NN}_1$ )	−32.6
$t_{(0,0,1)}$ ( $\text{NN}_2$ )	−4.5
$t_{(1,1/2,1/2)}$ ( $\text{NN}_3$ )	5.6
$t_{(1,0,1)}$ ( $\text{NN}_4$ )	3.9
Standard deviation	24.3

To test these predictions, we calculated—via linear-response theory and Monte Carlo simulations—the Curie temperature  $T_C$  of a set of  $\text{Ga}_{30}\text{Mn}_2\text{As}_{32}$  cubic supercells, where the two Mn substitutional impurities occupy different sites in the cation sublattice, separated by the fcc lattice vector  $\mathbf{R}$ . We find that  $T_C$  increases from 189 K when  $\mathbf{R} = \text{NN}_1$ , to 206 K for  $\mathbf{R} = \text{NN}_2$ , and to 289 K for  $\mathbf{R} = \text{NN}_4$ . These results confirm the predictions of our ‘data mining’ approach (table 2) that  $T_C$  anti-correlates with the number of first-nearest-neighbour Mn pairs.



interactions  $\{J_{ij}\}$  in a specific configuration  $\sigma$  may be misleading. Indeed, the exchange interactions  $\{J_{ij}\}$ —which depend not only on  $i$  and  $j$ , but also on the position of spectator ions [3, 4]—are merely inputs to a Monte Carlo simulation of the Heisenberg Hamiltonian that produces  $T_C$ . It is the *complete* set of exchange interactions  $\{J_{ij}\}$  for a given configuration  $\sigma$  that decides  $T_C(\sigma)$ .

The failure to rationalize  $T_C$  in terms of the contribution of specific, individual exchange interactions  $J_{ij}$ s suggests considering the exchange interactions between clusters as the source of the dependence of  $T_C$  on  $\{N_R\}$ . It has been observed [12, 13] that, by virtue of the strong ferromagnetic coupling between nearest-neighbour Mn ions, each Mn NN<sub>1</sub> pair acts as a single magnetic centre Mn<sub>2</sub>. At fixed Mn concentration, the average distance between magnetic centres increases when the Mn ions are clustered in pairs, compared to the case where the Mn ions are homogeneously dispersed. As a result, even though the total spin of a Mn cluster is larger than the spin of an isolated Mn ion, the exchange interactions between such clusters decrease, leading to an overall decrease in  $T_C$ . This argument also implies that, when the Mn ions are clustered in pairs, the percolative concentration threshold—i.e. the minimum Mn concentration below which ferromagnetism cannot occur due to the absence of magnetic percolation—increases.

When larger Mn clusters are formed, for example following spinodal decomposition of the (Ga, Mn)As alloy, the behaviour of  $T_C$  depends crucially on the clusters' shape, size and spatial distribution, which are often determined by non-equilibrium decomposition dynamics. In [11] we showed that the presence of short-range order in the Ga<sub>0.92</sub>Mn<sub>0.08</sub>As alloy (8% Mn concentration) leads to a significant decrease in  $T_C$  compared to the homogeneous random alloy, because the resulting Mn-rich clusters are only very weakly coupled (super-paramagnetism). For higher Mn concentrations, however, it is possible that the Mn-rich clusters could be strongly magnetically coupled, leading to an increase in  $T_C$  with respect to the homogeneous random alloy of the same Mn concentration. An example of this behaviour was given by Katayama-Yoshida *et al* [14] in the case of the Ga<sub>0.70</sub>Cr<sub>0.30</sub>N alloy.

Chang *et al* [15] recently suggested that, in addition to carrier-induced magnetic interactions, Mn–Mn first-nearest-neighbour pairs are coupled by superexchange interactions, which favour an anti-ferromagnetic spin alignment. They estimated that, in the absence of hole carriers, the ferromagnetic spin configuration of a random (Ga, Mn)As alloy with  $x_{\text{Mn}} = 6.25\%$  would be 2.77 meV higher in energy than the spin-glass configuration. However, this energy difference is much smaller than the ferromagnetic stabilization energy induced by hole carriers in uncompensated (Ga, Mn)As alloys [6]. Indeed, Chang *et al* [15] showed that the Curie temperature of the (Ga, Mn)As random alloy changes very little when superexchange interactions are included.

In conclusion, we have demonstrated—via a statistical analysis of first-principles calculations of the Curie temperature—that the most relevant design parameter to achieve high  $T_C$  in Mn-doped GaAs is the concentration of Mn–Mn first-nearest-neighbour pairs. Reducing the occurrence of such pairs would lead to a significant increase in the  $T_C$  of (Ga, Mn)As alloys. Since it is energetically favourable for Mn substitutional impurities in GaAs to form nearest-neighbour pairs [16, 17], reducing the concentration of such pairs may require non-equilibrium growth techniques or atom-by-atom manipulation of the Mn impurities [5].

### Acknowledgments

This work was supported by the US Defense Advanced Research Projects Agency (DARPA), the Defense Sciences Office, under the National Renewable Energy Laboratory (NREL) contract no. DEAC36-99-GO10337. MvS was supported by the Office of Naval Research (ONR) contract N00014-02-1-1025.

## References

- [1] Cheng C, Needs R J, Heine V and Jones I L 1989 *Phase Transit.* **16/17** 263
- [2] Zunger A and Mahajan S 1994 *Handbook of Semiconductors* vol 3 (Amsterdam: Elsevier) p 1399
- [3] Franceschetti A, Dudiy S V, Barabash S V, Zunger A, Xu J and van Schilfgaarde M 2006 *Phys. Rev. Lett.* **97** 047202
- [4] Xu J L, van Schilfgaarde M and Samolyuk G D 2005 *Phys. Rev. Lett.* **94** 097201
- [5] Kitchen D, Richardella A, Tang J M, Flatté M E and Yazdani A 2006 *Nature* **442** 436
- [6] Mahadevan P, Zunger A and Sarma D D 2004 *Phys. Rev. Lett.* **93** 177201
- [7] Samarth N 2006 *Nature* **442** 359
- [8] Zunger A 1994 *NATO ASI on Statics and Dynamics of Alloy Phase Transformations* (New York: Plenum)
- [9] van Schilfgaarde M and Antropov V P 1999 *J. Appl. Phys.* **85** 4827
- [10] Matsukura F, Ohno H, Shen A and Sugawara Y 1998 *Phys. Rev. B* **57** R2037
- [11] Franceschetti A, Barabash S V, Osorio-Guillen J, Zunger A and van Schilfgaarde M 2006 *Phys. Rev. B* **74** 241303
- [12] Raebiger H, Ayuela A and von Boehm J 2005 *Phys. Rev. B* **72** 014465
- [13] Raebiger H, Hynninen T, Ayuela A and von Boehm J 2006 *Physica B* **376** 643
- [14] Katayama-Yoshida H, Sato K, Fukushima T, Toyoda M, Kizaki H, Dinh V A and Dederichs P H 2007 *Phys. Status Solidi a* **204** 15–32
- [15] Chang Y H, Park C H, Sato K and Katayama-Yoshida H 2006 *J. Korean Phys. Soc.* **49** 203
- [16] van Schilfgaarde M and Mryasov O N 2001 *Phys. Rev. B* **63** 233205
- [17] Mahadevan P, Osorio-Guillen J and Zunger A 2005 *Appl. Phys. Lett.* **86** 172504